AIP Conference Proceedings

Simulation of tantalum nanocrystals under shock-wave loading: Dislocations and twinning

Cite as: AIP Conference Proceedings **1793**, 070002 (2017); https://doi.org/10.1063/1.4971590
Published Online: 13 January 2017

D. R. Tramontina, E. N. Hahn, M. A. Meyers, et al.


View Online


Export Citation

ARTICLES YOU MAY BE INTERESTED IN

Atomistic shock Hugoniot simulation of single-crystal copper
Journal of Applied Physics **96**, 3793 (2004); https://doi.org/10.1063/1.1789266

Influence of defects on the shock Hugoniot of tantalum
Journal of Applied Physics **125**, 215902 (2019); https://doi.org/10.1063/1.5096526

Non-equilibrium molecular dynamics simulations of spall in single crystal tantalum
AIP Conference Proceedings **1793**, 070006 (2017); https://doi.org/10.1063/1.4971594

Lock-in Amplifiers up to 600 MHz
Zurich Instruments
Watch

AIP Publishing

© 2017 Author(s).

Simulation of Tantalum Nanocrystals Under Shock-Wave Loading: Dislocations and Twinning

D.R. Tramontina[1,2,3], E. N. Hahn[4], M.A. Meyers[4], and E.M. Bringa[1,3,a]

[1]*Facultad de Ciencias Exactas y Naturales, National University of Cuyo, Mendoza M5502JMA, Argentina.*
[2]*Engineering Faculty, University of Mendoza, Mendoza M5502BZG, Argentina.*
[3]*CONICET, Argentina.*
[4]*University of California San Diego, La Jolla, CA 92093, USA.*
[a]Corresponding author: ebringa@yahoo.com

Abstract. We simulate strong shock waves in nanocrystalline tantalum using atomistic molecular dynamics simulations, for particle velocities in the range 0.35-2.0 km s^{-1}, which induce pressures in the range 20-195 GPa. Our simulations explore strain rates in the range 10^8 s^{-1} - 10^{10} s^{-1}, and lead to a peak strength in the range 3-15 GPa. Nanocrystalline tantalum exposed to strong shock waves demonstrates deformation enabled by concomitant dislocations, twinning, and grain boundary activity at a variety of particle velocities. Twinning is observed for a mean grain size of 7 nm, starting at around 32 GPa, in disagreement with models which predict a Hall-Petch behavior for twinning, i.e. a twinning stress scaling with grain size d as $d^{-0.5}$, and supporting the presence of an inverse Hall-Petch effect for twinning at small grain sizes.

Introduction

Tantalum (Ta) is a model body-centered cubic (bcc) metal with excellent phase stability under large pressures and at high temperatures [1,2]. Strong phase stability compared to other bcc metals, such as iron [3], provides a direct route to evaluate bcc plasticity without phase transformations. The bcc phase, in general, displays increased temperature and strain-rate dependence of strength. Within the nanocrystalline regime, we can expect an increase in strength owing to manifestations of several grain size dependent deformation mechanisms [1]. Of direct interest here is the observation of grain size and shock strength dependent twinning. Previous work has already shown that the prevalence of twinning is highly anisotropic [4,5].

Materials And Methods

Our simulation samples were generated through an in-house Voronoi tessellation code. Grain size can be controlled by selecting an appropriate number of grain centers for a given box dimension. The grain texture is defined randomly. In the present case, our average crystallite size is ~7 nm with total dimensions of 35x35x125 (nm^3) corresponding to about 8 million atoms. Periodic boundary conditions were applied to the transverse directions and the back region allows for free surface release. Most simulations were run at low temperatures (10 K) to simplify defect detection.

We use the LAMMPS molecular dynamics simulation code [6] with an embedded atom method potential developed by Ravelo *et al.* [5]. A rigid piston is employed for the generation of the shock wave, moving at an imposed particle velocity (U_p) [7]. An ideal shock wave is typically applied as a perfect square signal, with zero rise time (t_r). Experimental shocks, on the other hand, are typically applied with rise times as long as a nanosecond [8]. For this reason, we use a 15 ps linear velocity ramp to investigate velocities in the range U_p = 0.35 - 2 km s^{-1}.

Shock Compression of Condensed Matter - 2015
AIP Conf. Proc. 1793, 070002-1–070002-6; doi: 10.1063/1.4971590
Published by AIP Publishing. 978-0-7354-1457-0/$30.00

The deviatoric shear stress was calculated using equation #1 in [9]. The Crystal Analysis Tool (CAT) [10] was employed for strain and structure-type calculations. Primary visualization and rendering were accomplished with Ovito [11]. MDRender [5] implemented within SPaSM [12] was used to perform simulated crystallographic orientation imaging microscopy (OIM) for comparison with CAT/OVITO.

Results

The shock wave particle velocity was varied to cover the range from 0.35 to 2 km s^{-1}. Figure 1 shows selected snapshots of a lateral view, 35 ps after the shock wave was initiated traveling from left to right in the views. Atoms in this sample were colored following their Common Neighbor Analysis (CNA) signature. Blue color was assigned to atoms with a BCC structure whilst green was assigned to atoms of unidentified arrangement. An unshocked reference sample is shown in fig. 1(a) and was used in coordination with the shocked specimens in order to virtually track the evolution of defects shown in the other frames. For method reliability purposes, our tracking method was performed by means of the structure matching algorithms in CAT [10].

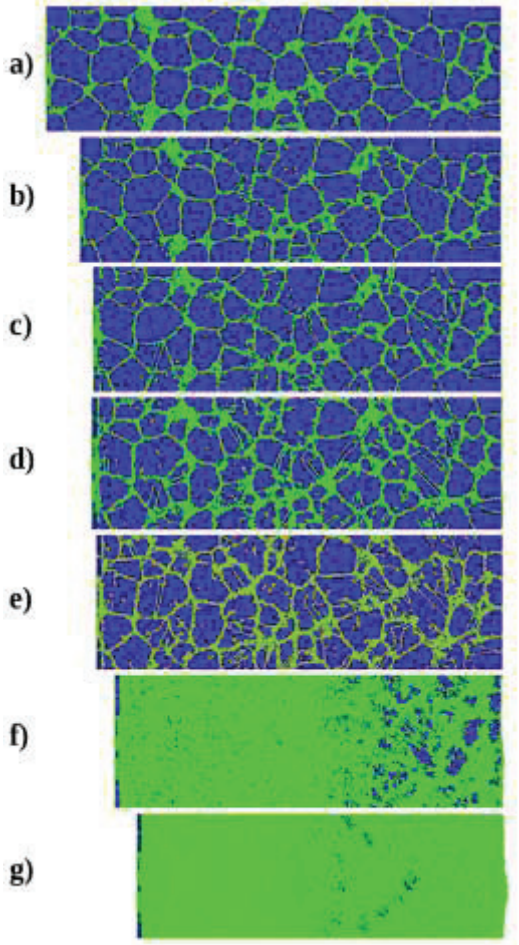

FIGURE 1. View of nanocrystalline Tantalum samples, shocked at several velocities. Shock motion goes from left to right, 35 ps after shock started. a) Unshocked sample, b) U_p=0.35 km s^{-1}, c) U_p=0.5 km s^{-1}, d) U_p=0.75 km s^{-1}, e) U_p=0.88 km s^{-1}, f) U_p=1.5 km s^{-1}, g) U_p=2.0 km s^{-1}. Blue: BCC atoms; Green: Other atoms.

For particle velocities between 0.35 and 0.88 km/s (corresponding to fig. 1(b-e)), t = 35 ps corresponds nearly to the arrival of the shock at the rear surface. Figure 1(f,g) shows irregular aspects of the sample bottoms, represented by the right side of of both figures in this lateral view, indicating that tensile reflection of the shock wave has begun. At U_p= 0.35 km s^{-1} (P ~ 20 GPa) no twins are present. Instead, some slight grain boundary activity

and vacancy motion is present, along with dislocation nucleation from grain boundaries. Heterogeneous dislocation nucleation in defective single crystals shocked along [001] was found to start at P=12 GPa [9].

At U_p= 0.5 km s^{-1} (P ~ 32 GPa) twin nucleation is observed along with the previously commented deformation mechanisms. This twinning threshold is similar to the one found for defective single crystals shocked along [001] by Tramontina et al. [9]. In the 2D projection shown in Fig. 1, twins appear as green intragranular loops. Defect density increases with particle velocity as expected with coexistence and competition between grain boundary sliding; vacancy nucleation and motion; dislocation nucleation and motion; and twin nucleation and growth. Maximum deviatoric shear stress for U_p=0.5 km s^{-1} was found to be in the range 4~5 GPa, enough to trigger twinning. At U_p= 1.5 km s^{-1} and above, the high deformation state limits the capacity of the CNA filter for structure identification.

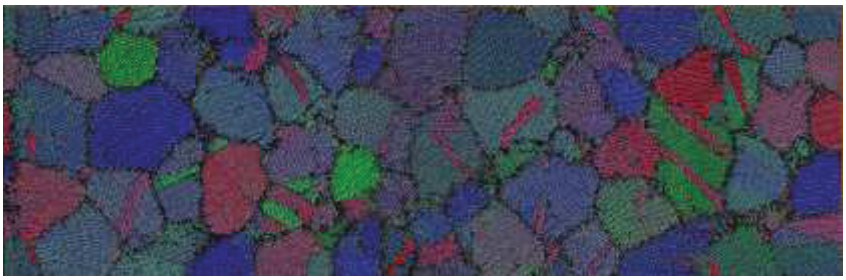

FIGURE 2. Simulated OIM analysis performed in a sample for U_p=0.75 km s^{-1}, 35 ps after shock initiation. Different colors indicate different crystal orientations. This is the same snapshot in fig. 1(d). Twinning appears in several grains, as more than one crystalline orientation within a given grain.

Twins can be visualized by their boundaries surrounding a new lenticular "grain" when a CNA filter is applied. The same snapshot in fig. 1(c) was processed using simulated OIM for comparison purposes. Results are displayed in fig. 2, where color is assigned by crystallite orientation, confirming intragranular twinning in several nanograins of varying orientation.

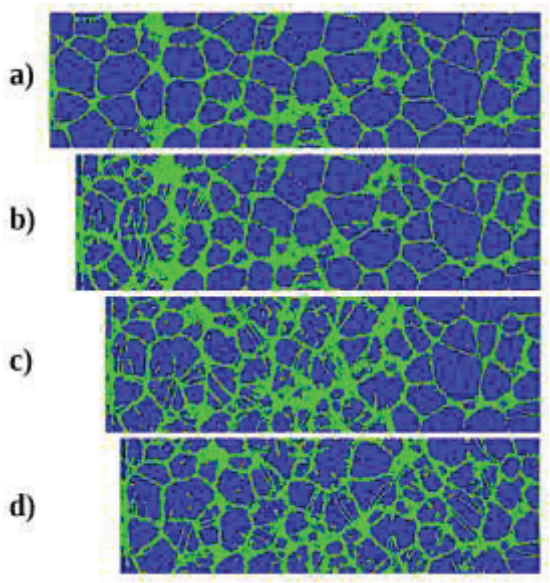

FIGURE 3. Sequence of snapshots for a shock with U_p=0.75 km s^{-1} . Shock motion goes from left to right, a) t= 5 ps, b) t= 15 ps, c) t= 25 ps, d) t= 35 ps. Blue: BCC atoms; Green: Other atoms.

Figure 3 shows a sequence of snapshots for U_p=0.75 km s^{-1}, displaying several grains with twins, which remain stable during the simulation. Longer simulations might lead to detwinning during loading, as observed for

single crystal simulations [5]. This particle velocity corresponds with the profiles in the left of Fig. 4. Figure 4 (c) shows that peak shear values reach ~ 5 GPa on the shock wave front. This value is enough for plasticity initiation, and results in a transition from a uniaxial strain state to a more three dimensional strain state. This transition is responsible for the decay of shear stress measured in the trailing portion of the shock wave.

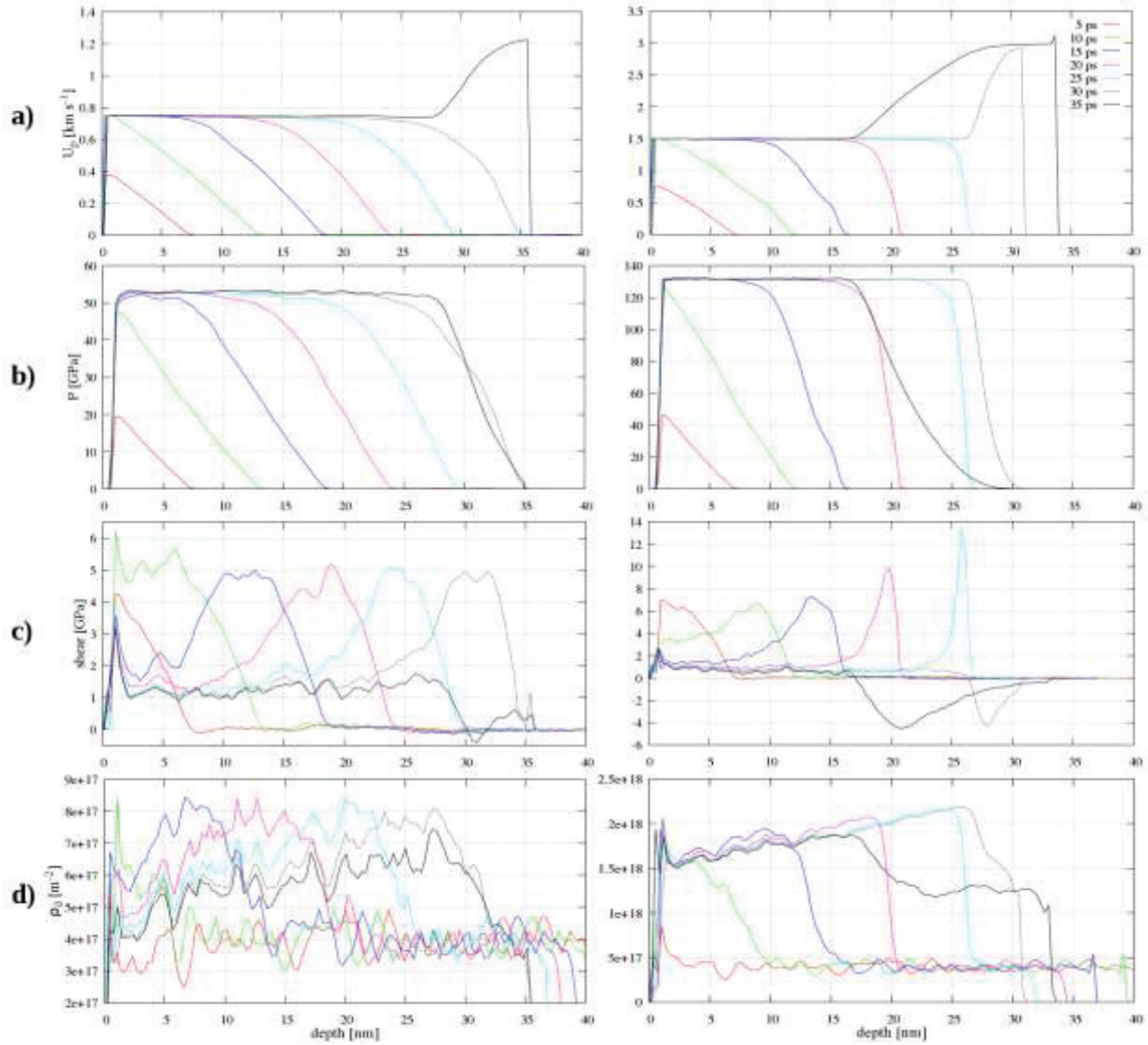

FIGURE 4. Profile evolution for shocks at U_p=0.75 km s^{-1} (left panel) and U_p=1.5 km s^{-1} (right panel).

Figure 4 shows selected profiles for two particle velocities: 0.75 km s^{-1} in the left panel, and 1.5 km s^{-1} on the right. Quantities were measured as a function of distance along the shock direction. Particle velocity is depicted in fig. 4(a), where the linear profile of the shock front and rise-time is clearly shown. A reflexion is produced in the last frames as the shock bounces back from the bottom of the sample. Figure 4(c) show the deviatoric shear stress for both particle velocities. In the left column, fig. 4(c) shows a maximum peak shear of ~ 5 GPa. When the piston velocity is increased to 1.5 km s^{-1} as shown in the right plot of fig. 4(a), the sample is no longer able to accommodate the shear stress by plasticity-based relaxation, so new peak values are reached as the shock moves through the sample, and reaches a value of ~ 14 GPa just before the back-surface reflexion. We note that, for a given

particle velocity, the resulting pressures are similar to the ones found for single crystal shocks by Ravelo *et al.* [5], and Tramontina *et al.* [9].

Summary and Conclusions

Our simulations of shocks in nanocrystalline Ta expand the monocrystalline results by Ravelo et al [5] and Tramontina et al [9] on shock propagation in single crystal Ta. Our simulations explore strain rates in the range 10^8 s^{-1} - 10^{10} s^{-1}, and lead to a peak strength in the range 3-15 GPa, in agreement with recent experiments in micron-sized polycrystals and reaching sub-micron grain sizes [13]. The flow stress well behind the shock front is around 1 GPa, similar to the single crystal case [9].

Nanocrystals offer various pathways for plasticity thanks to their complex structure. Plasticity detection and quantification can be extremely challenging due to the presence of evolving dislocation networks in certain grain boundaries, along with large strain states and possibly immense defect densities. Our simulations of shocks in nanocrystalline Ta, with a mean grain size of 7 nm, show coexistence of mechanisms such as grain boundary activity, dislocations, and twinning, similar to what was discussed for shocks in f.c.c. nanocrystals [7]. Grain boundary sliding and reaccommodation is observed at all shock pressures. Dislocation nucleation from grain boundaries is also observed starting at the lowest simulated pressure, and requires relatively low stress. Homogeneous dislocation nucleation is not expected for Ta single crystals [9], and would not play a role in nanocrystals. Twinning, identified both by Common Neighbor Analysis (CNA) and simulated Orientation Image Microscopy (OIM), starts at about 32 GPa, in agreement with some experiments in single crystals [14] and at larger pressure than twinning in micron-size polycrystals [15].

In our simulations twinning is possible even for grain sizes as small as 7 nm, as opposed to the suggestion by Lu *et al.* [16], who predicted a Hall-Petch behavior of the twinning nucleation barrier which effectively eliminated twinning for grain sizes below ~70 nm, based on the lack of twinning in their experiments. Recently, Meyers *et al.* [17] proposed an inverse Hall-Petch behavior for grain sizes below 70 nm in agreement with our observations.

Twinning in single and polycrystals is a complex phenomena, and it can play a central role in failure and spall [18,19]. This preliminary study has to be extended to larger grain sizes to uncover the nature of a possible inverse Hall-Petch effect. Simulated shock recovery studies [20] would allow improved comparison with experiments including microscopy of recovered samples, since detwinning could be significant [14,16].

Acknowledgments

DRT and EMB thank support from CONICET, PICT2008-1325, and a SeCTyP-UNCuyo grant. ENH and MAM were supported by the UC Research Laboratories Grant and DOE SSAP. ENH also received support from DOE ASCR.

References

1. E.H. Hahn, M.A Meyers, *Mat. Sci. Eng. A* **646** (2015): 101-134.
2. L. Burakovsky, S.P. Chen *et al*, *Phys. Rev. Lett.* **104** (2010) 255702.
3. N. Gunkelmann, D.R. Tramontina, E.M. Bringa, H. Urbassek, *New J. Phys.* **16** (2014) 093032.
4. J.N. Florando, N.T. Barton *et al., J. Appl Phys.* **113** (2013) 083522.
5. R. Ravelo, T.C. Germann *et al., Phys. Rev. B* **88** (2013) 134101.
6. S. Plimpton, *J. Comp. Phys.* **117-1** (1995) 1.
7. E. M. Bringa, *et al.*, *Science* **309** (2005) 1838–1841.
8. D. Milathianaki *et al., Science* **342** (2013) 220–223.
9. D. R. Tramontina *et al., High Energy Density Physics* **10** (2014) 9–15.
10. A. Stukowski, K. Albe, *Modelling Simul. Mater. Sci. Eng.* **18** (2010) 085001.
11. A. Stukowski, *Modelling Simul. Mater. Sci. Eng.* **18** (2010) 015012.
12. K. Kadau, T.C. Germann, P.S. Lomdahl, Int. J. Mod. Phys. C 17 (2006) 1755–1761.
13. H.-S. Park *et al., Phys. Rev. Lett.* **114,** (2015) 065502.
14. C. H. Lu *et al., Acta Materialia* **60** (2012) 6601–6620.
15. L. E. Murr *et al.*, *Acta Materialia* **45** (1997) 157–175.

16. C. H. Lu *et al., Acta Materialia* **61** (2013) 7767–7780.
17. Y. Tang, E. M. Bringa, M. A. Meyers, *Materials Science and Engineering: A* **580** (2013) 414–426.
18. J. P. Escobedo, E. K. Cerreta, D. Dennis-Koller, *JOM* **66,** 156–164 (2013).
19. E. N. Hahn *et al.*, AIP Conf. Proc. (2015) (Submitted, SCCM: MS #C5.4-15-1224)
20. H. N. Jarmakani *et al., Acta Materialia* **56** (2008) 5584–5604.